Mutational Analysis of Metallo-β-lactamase CcrA from *Bacteroides fragilis*[†]

Margaret P. Yanchak, Rebecca A. Taylor, and Michael W. Crowder*

Department of Chemistry and Biochemistry, 112 Hughes Hall, Miami University, Oxford, Ohio 45056

Received May 9, 2000; Revised Manuscript Received June 30, 2000

ABSTRACT: In an effort to evaluate the roles of Lys184, Asn193, and Asp103 in the binding and catalysis of metallo-β-lactamase CcrA from *Bacteroides fragilis*, site-directed mutants of CcrA were generated and characterized using metal analyses, CD spectroscopy, and kinetic studies. Three Lys184 mutants were generated where the lysine was replaced with alanine, leucine, and glutamate, and the analysis of these mutants indicates that Lys184 is not greatly involved in binding of cephalosporins to CcrA; however, this residue does have a significant role in binding of penicillin G. Three Asn193 mutants were generated where the asparagine was replaced with alanine, leucine, and aspartate, and these mutants exhibited <4-fold decrease in k_{cat}, suggesting that Asn193 does not play a large role in catalysis. However, stopped-flow visible kinetic studies showed that the Asn193 mutants exhibit a slower substrate decay rate and no change in the product formation rate as compared with wild-type CcrA. These results support the proposed role of Asn193 in interacting with and activating substrate during catalysis. Two Asp103 mutants were generated where the aspartate was replaced with serine and cysteine. The D103C and D103S mutants bind the same amount of Zn(II) as wild-type CcrA and exhibited a 10^2-fold and 10^5-fold decrease in activity, respectively. Results from solvent isotope, proton inventory, and rapid-scanning visible studies suggest that Asp103 plays a role in generating the enzyme intermediate but does not donate a proton to the enzyme intermediate during the rate-limiting step of the catalytic mechanism.

The metallo-β-lactamases are a class of bacterial enzymes that hydrolyze and inactivate all known penicillins, cephalosporins, and carbapenems, rendering a bacterium resistant to the largest group of clinically useful antibiotics. To date, greater than 20 bacterial strains are known to produce a metallo-β-lactamase, and many of these bacteria are minor pathogens (*1, 2*). Bush has classified the metallo-β-lactamases into three subgroups, based upon amino acid sequence comparisons (*1*), and this scheme appears best to broadly classify the metallo-β-lactamases in terms of structure. The subgroup Ba enzymes require two Zn(II) ions for full catalytic activity, prefer penicillins as substrates, and have monomeric molecular masses of 26−27 kDa. The metallo-β-lactamases CcrA from *Bacteroides fragilis* (*3, 4*) and β-lactamase II from *Bacillus cereus* (*5, 6*) are prototypical members of this subgroup. The subgroup Bb enzymes require one Zn(II) for full activity and prefer carbapenems as substrates. The metallo-β-lactamase AE036 from *Aeromonas hydrophila* is a representative member of this subgroup (*7, 8*). Subgroup Bc contains only the metallo-β-lactamase L1 from *Stenotrophomonas maltophilia*. L1 is distinct in that it is 4−5 kDa larger than the other metallo-β-lactamases, contains a metal binding ligand motif unlike the other enzymes, exhibits the least amino acid sequence homology with the other metallo-β-lactamases, and exists as a tetramer in solution (*9, 10*). Alarmingly, inhibition studies with nonclinical inhibitors have shown large differences in inhibitory efficacies between the metallo-β-lactamases from different classes, suggesting that one inhibitor may not inhibit all metallo-β-lactamases (*11*−*13*).

One of the best-studied metallo-β-lactamases is CcrA from *B. fragilis*. Concha et al. reported the crystal structure of CcrA in 1996 (*4*), and since then, several other structures have been reported of the enzyme with competitive inhibitors bound within the active site (*14, 15*). Solution NMR studies have also been reported on CcrA (*16, 17*). Since it has been impossible so far to determine the crystal structure of CcrA with substrate bound in the active site, modeling studies have been used to propose how substrate binds to the enzyme. These modeling studies were based on three key assumptions: (1) the bridging hydroxide was assumed to be the nucleophile during catalysis, and any docked substrate was assumed to have its β-lactam carbonyl near this bridging group; (2) the invariant carboxylate on substrate was assumed to form an electrostatic interaction with Lys184; and (3) the β-lactam carbonyl oxygen was assumed to form an H-bond with Asn193 and Zn_1 (*4*). Asn193 and Zn_1 were predicted to activate the β-lactam carbonyl for nucleophilic attack. Interestingly, Toney and co-workers have reported the crystal structures of CcrA with bound competitive inhibitors (*14, 15*), and both studies identified Asn193 and Lys184 as making significant contacts with the inhibitors.

Recently, Wang and Benkovic have identified an intermediate that is formed during the CcrA-catalyzed hydrolysis of nitrocefin (*18, 19*). Pre-steady-state kinetic studies were used to demonstrate that the decay of this intermediate is rate limiting, and Benkovic and co-workers have postulated that the intermediate is a ring-opened form of nitrocefin with

[†]Supported by NIH Grant R29 AI40052 (to M.W.C.) and by a 1999 Miami University Committee on Undergraduate Research Award (to R.A.T.). R.A.T. was a 1999 University Summer Scholar.

* Correspondence should be addressed to this author. Phone: (513) 529-7274, fax: (513) 529-5715, e-mail: crowdemw@muohio.edu.

10.1021/bi0010524 CCC: $19.00
Published on Web 08/18/2000

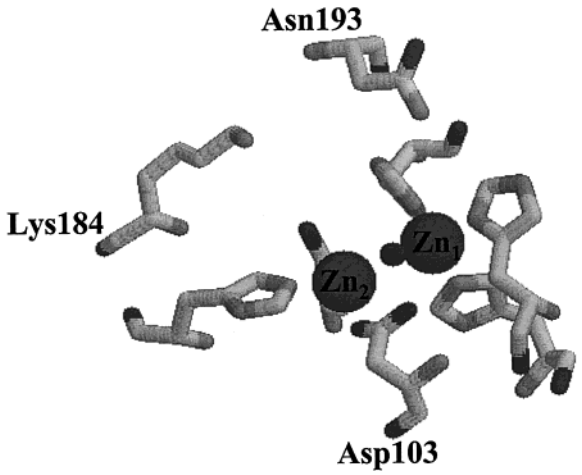

FIGURE 1: Schematic view of amino acid residues mutated in this study and their proximity to the dinuclear Zn(II) center in metallo-β-lactamase CcrA. This figure was rendered using RasMol v. 2.6 (R. Sayle, 1994, Greenford, Middlesex, U.K.).

an anionic nitrogen (*18*−*20*). Solvent isotope studies were used to show that a proton transfer occurs during a rate-significant step, and the protonation of intermediate was postulated to be the rate-limiting chemical event (*18, 21*). The origin of this proton is currently unknown; however, several groups have proposed that either the Zn(II)-binding Asp103 might donate a proton to the intermediate during the rate-limiting step or the proton in flight originates from solvent (*4, 11, 20*).

To probe the roles of Lys184 in substrate binding, Asn193 in substrate binding and catalysis, and Asp103 in catalysis, site-directed mutagenesis studies were conducted (Figure 1). These mutants were characterized using metal analyses, CD[1] spectroscopy, and pre-steady-state and steady-state kinetics. The results presented herein allow for a more refined model for substrate binding to CcrA.

EXPERIMENTAL PROCEDURES

Materials. E. coli strains DH5α and BL21(DE3) were obtained from Gibco BRL and Novagen, respectively. The plasmid pMSZ02 was generously supplied by Wang and Benkovic (*18*) and consists of pET27b with the *ccrA* gene (TAL 3636) (*3, 22*) ligated between *Nde*I and *Bam*HI sites. pET27b and pUC19 were purchased from Novagen. Primers for sequencing and mutagenesis studies were purchased from National Biosciences, Inc., or Integrated DNA Technologies. Deoxynucleotide triphosphates (dNTP's), $MgSO_4$, thermopol buffer, Deep Vent DNA polymerase, and restrictions enzymes were purchased from Promega or New England Biolabs. Polymerase chain reaction was conducted using a Thermolyne Amplitron II unit. DNA was purified using the Qiagen QIAQuick gel extraction kit or Plasmid Purification kit with QIAGEN-tip 100 (Midi) columns. Wizard Plus Minipreps were acquired from Promega. Luria−Bertani (LB) medium was made following published procedures (*23*). Isopropyl-β-thiogalactoside (IPTG), Biotech grade, was procured from Fisher Scientific or GOLD Biotechnology. Phenylmethylsulfonyl fluoride (PMSF) was purchased from Sigma. A Minitan II concentrator system was purchased from Fisher Scientific and was equipped with four 10 000 NMWL plates from Millipore. Protein solutions were concentrated with an Amicon ultrafiltration cell equipped with YM-10 DIAFLO membranes from Amicon, Inc. Dialysis tubing was prepared using Spectra/Por-regenerated cellulose molecular porous membranes with a molecular mass cutoff of 6000−8000 g/mol. Metal-free buffers were prepared by treatment of buffers with Chelex 100 resin, purchased from Bio-Rad Laboratories, and filtration of the buffer through a 0.22 μm membrane from Osmonics, Inc. Q-Sepharose Fast Flow was purchased from Amersham Pharmacia Biotech. Nitrocefin was purchased from Becton Dickinson, and solutions of nitrocefin were filtered through a Fisherbrand 0.45 μm syringe filter. All buffers and media were prepared using Barnstead NANOpure ultrapure water.

Table 1: List of Primers (5′→ 3′) Used To Generate Mutants, with Nondegenerate Bases Listed in Boldface Type

primer	sequence
pUCMSZfor	CTATgCggCATCAgAgCAgATT
M13rev	gATAACAATTTCACACAggA
D103Cfor	CACTggCACggC**Tg**TTgTATTggCggA
D103Crev	TCCgCCAATACAA**CA**gCCgTgCCAgTg
D103Sfor	CACTggCACggC**Ag**TTgTATTggCggA
D103Srev	TCCgCCAATACAA**CT**gCCgTgCCAgTg
K184Afor	ATgTATgCTT**gC**AgACAACCAgg
K184Arev	CCTggTTgTCT**gC**AAgCATACAT
K184Efor	ATgTATgCTT**g**AAgACAACCAgg
K184Erev	CCTggTTgTCTT**C**AAgCATACAT
K184Lfor	ATgTATgCTT**CT**AgACAACCAgg
K184Lrev	CCTggTTgTCT**Ag**AAgCATACAT
N193Afor	ACAAgCATCggC**gC**CATCTCggACgC
N193Arev	gCgTCCgAgATg**gC**gCCgATgCTTgT
N193Dfor	ACAAgCATCggC**g**ACATCTCggACgC
N193Drev	gCgTCCgAgATgT**C**gCCgATgCTTgT
N193Lfor	ACAAgCATCggC**CT**CATCTCggACgC
N193Lrev	gCgTCCgAgATg**Ag**gCCgATgCTTgT

[1] Abbreviations: AMP, ampicillin; bp, base pair(s); CD, circular dichroism; dNTP's, deoxynucleotide triphosphates; ϵ, extinction coefficient; HEPES, 4-(2-hydroxymethyl)-1-piperazineethanesulfonic acid; ICP-AES, inductively coupled plasma with atomic emission spectroscopy; IPTG, isopropyl-β-D-thiogalactopyranoside; k_{cat}, turnover number; K_m, Michaelis constant; LB, Luria−Bertani; MTEN, buffer with 50 mM MES, 25 mM Tris, 25 mM ethanolamine, pH 7.0, containing 100 mM NaCl; PAGE, polyacrylamide gel electrophoresis; PCR, polymerase chain reaction; SDS, sodium dodecyl sulfate; Tris, tris-(hydroxymethyl)aminomethane.

By using the degenerate oligonucleotides in Table 1, Deep Vent polymerase, pMSZ03 as template, and polymerase chain reaction (PCR), mutant DNA was generated as described by Ho et al. (*24*). After PCR, the 830 bp DNA fragment containing the mutation was gel-purified, digested

with *Nde*I and *Bam*HI, and ligated into pUC19. The *ccrA* gene-containing plasmid was electroporated into *E. coli* DH5α cells. The subsequent cell suspension was plated onto LB-agar plates containing 100 μg/mL ampicillin and incubated overnight at 37 °C. DNA minipreps were performed on 10−20 of the colonies, and after incubation with either *Nde*I or *Bam*HI, electrophoresis was used to screen for colonies containing the correct size plasmid (3.3 kb). A colony with the appropriately sized plasmid DNA was subjected to large-scale plasmid purification, and a restriction map of the resulting purified plasmid was used to confirm further that the correct plasmid was isolated. DNA sequencing of the mutated *ccrA* gene using M13for and M13rev as the primers was used to confirm the presence of the mutation and that no other, unintended mutations were present in the gene.

The purified plasmid was digested with *Nde*I and *Bam*HI, and the *ccrA* gene was ligated into predigested pMSZ02. The resulting plasmid was transformed into *E. coli* DH5α cells, and the cell suspension was plated onto LB-agar plates containing 25 μg/mol kanamycin. DNA minipreps were performed on 10−20 of the resulting colonies, and, following incubation with either *Nde*I or *Bam*HI, electrophoresis was used to identify colonies with the correct size plasmid (6.1 kb). Large-scale DNA samples were prepared on one of the colonies containing DNA of the correct size, and the resulting plasmid DNA was sequenced (Biosynthesis and Sequencing Facility, Johns Hopkins University, Baltimore, MD) to check for any unwanted mutations in the DNA sequence.

Overexpression and Purification of Wild-Type CcrA and Its Mutants. Wild-type pMSZ02 and mutant forms of pMSZ02 were overexpressed using the procedure of Wang and Benkovic (*18*). The overexpressed proteins were purified using a single Q-Sepharose column (20 × 200 mm) as described previously (*18*).

Metal Content. The concentrations of wild-type CcrA and the mutants were determined by measuring the proteins' absorbance at 280 nm and using the published extinction coefficient of $\epsilon_{280\ nm} = 39\ 000\ M^{-1}\cdot cm^{-1}$ (*18*). Before metal analyses, the protein samples were dialyzed versus 3 × 1 L of metal-free, 50 mM HEPES, pH 7.5, over 96 h at 4 °C. A Varian Inductively Coupled Plasma Spectrometer with atomic emission spectroscopy detection (ICP-AES) was used to determine the metal content of multiple preparations of wild-type CcrA and CcrA mutants. Calibration curves were based on three standards and had correlation coefficient limits of at least 0.9950. The final dialysis buffer was used as a blank. The emission line of 213.856 nm is the most intense for zinc and was used to determine the Zn content in the samples. The errors in metal content data reflect the standard deviation (σ_{n-1}) of multiple enzyme preparations.

Steady-State Kinetic Studies. The hydrolysis of nitrocefin by CcrA and its mutants was monitored by detecting the formation of product at 485 nm, and absorbance data were converted into concentration data using a previously published extinction coefficient ($\Delta\epsilon = 17\ 400\ M^{-1}\cdot cm^{-1}$) (*25*). The hydrolysis of penicillin G was monitored by following the depletion of penicillin G at 235 nm, and absorbance data were converted into concentration data using the extinction coefficient $\Delta\epsilon = -936\ M^{-1}\cdot cm^{-1}$ (*10*). The hydrolysis of cephaloridine was monitored by following the depletion of cephaloridine at 265 nm, and absorbance data were converted into concentration data using the extinction coefficient $\Delta\epsilon = -6980\ M^{-1}\cdot cm^{-1}$ (*10*). The kinetic experiments were conducted on a Hewlett-Packard model 5480A UV−Vis spectrophotometer, at 25 °C. The buffer used in the kinetic studies was 1× MTEN buffer (50 mM MES, 25 mM Tris, 25 mM ethanolamine, pH 7.0, containing 100 mM NaCl). Substrate concentrations were varied between 0.1 and 10 × K_m, except in the studies using penicillin G and the mutants. pH dependence studies were completed with 1× MTEN buffer adjusted to pH 5.5 through pH 10.0 (*18*). The absorbance versus time data for reactions at pH 9.5 and 10.0 were corrected for background hydrolysis of substrate at these higher pH values in the absence of enzyme. Concentrations of product formed per second versus initial substrate concentration data were directly fitted to the Michaelis−Menten equation using Curve Fit in order to determine the steady-state kinetic constants k_{cat} and K_M. Reported errors for kinetic constants reflect standard deviations (σ_{n-1}) of multiple trials from two or more enzyme preparations.

Table 2: Metal Content for Wild-Type CcrA and Mutants of CcrA in Metal-Free, 50 mM HEPES, pH 7.0

mutant	metal content [mol of Zn(II)/mol of protein]
wild-type	1.5 ± 0.1
D103C	1.6 ± 0.2
D103S	1.7 ± 0.3
K184A	2.0 ± 0.1
K184E	1.5 ± 0.1
K184L	1.6 ± 0.1
N193A	1.4 ± 0.2
N193D	1.7 ± 0.3
N193L	1.4 ± 0.1

Proton inventory and solvent isotope studies were conducted in 1× MTEN buffer at pH 7.0. To prepare 1× MTEN in 100% D_2O, the buffer components were dissolved in D_2O, the pH of the solution was adjusted to pD 7.0 with DCl or NaOD, and the solution was lyophilized overnight. The lyophilized buffer components were redissolved in D_2O, and the solution was lyophilized a second time. After redissolving the buffer components a second time in D_2O, the pH of the solution was checked, and the buffer was used to make a stock solution of nitrocefin and for steady-state kinetic studies. The studies in 25%, 50%, and 75% D_2O were conducted by diluting the substrate and buffers in 100% D_2O with nitrocefin and buffers prepared in H_2O. Enzyme stocks in 100% D_2O buffer were prepared by dialyzing 1 mL of 200−400 μM protein versus 3 × 100 mL of 1× MTEN in D_2O, pD 7.0. Plots of k_{cat} versus % D_2O were generated, and the data were fitted to $k_{obs} = k_{cat}[1 - n + n(k^D/k^H)]$, where k_{obs} is the k_{cat} determined at each % D_2O, k_{cat} was determined from steady-state kinetic studies (Table 2), n is the % D_2O, k^D is k_{cat} determined in 100% D_2O, and k^H is k_{cat} determined in 0% D_2O buffer.

Pre-Steady-State Kinetic Studies. Pre-steady-state kinetic studies of the CcrA-catalyzed hydrolysis of nitrocefin were conducted in 1× MTEN, pH 7.0, at 25 °C on an SX.17MW stopped-flow system (Applied Photophysics, Leatherhead, United Kingdom), as previously described (*18*). Absorbance changes were monitored with either an Applied Photophysics PD.1 photodiode array detector or an absorbance photomultiplier at 390 nm (substrate disappearance) and 485 nm (product formation). Data from at least three reproducible experiments were collected, averaged, and corrected for the

Table 3: Steady-State Kinetic Constants for Hydrolysis of Nitrocefin, Penicillin G, and Cephaloridine by CcrA in 1× MTEN, pH 7.0

	nitrocefin		penicillin G		cephaloridine	
enzyme	K_m (μM)	k_{cat} (s^{-1})	K_m (μM)	k_{cat} (s^{-1})	K_m (μM)	k_{cat} (s^{-1})
wild-type	7.8 ± 1.3	216 ± 13	50 ± 2	99 ± 2	6.4 ± 0.9	54 ± 2
D103C	39 ± 9	1.9 ± 0.1	321 ± 54	3.3 ± 0.2	12 ± 2	0.16 ± 0.05
D103S		<0.003		<0.50		<0.005
K184A	4.8 ± 0.2	99 ± 4	1005 ± 257	174 ± 24	7.9 ± 1.3	83 ± 1
K184E	15 ± 2	100 ± 8	3941 ± 685	121 ± 16	25 ± 4	101 ± 6
K184L	4.2 ± 0.2	52 ± 1	628 ± 95	326 ± 23	18 ± 4	93 ± 3
N193A	7.2 ± 0.8	95 ± 8	149 ± 16	390 ± 17	39 ± 5	172 ± 9
N193D	5.1 ± 0.5	51 ± 2	469 ± 60	377 ± 20	20 ± 2	150 ± 4
N193L	21 ± 1	47 ± 1	756 ± 108	224 ± 13	115 ± 15	82 ± 5

instrument dead time of 1.5 ms. The absorbance data were converted to concentration data as described previously (*18, 26*). The corrected concentration versus time data were fitted to $y = y_o + ae^{-bx}$ for substrate disappearance and to $y = y_o + a(1 - e^{-bx})$ for product formation using CurveFit v. 4.0 (*26*).

Circular Dichroism. Circular dichroism samples were prepared by dialyzing the purified enzyme samples versus 3 × 2 L of 5 mM phosphate buffer, pH 7, over 6 h. The samples were diluted with final dialysis buffer to ~75 μg/mL. A JASCO J-710 CD spectropolarimeter operating at 22 °C was used to collect CD spectra.

RESULTS

Overexpression and Purification of Wild-Type CcrA and CcrA Mutants. Eight mutants of CcrA (K184A, K184L, K184E, N193A, N193L, N193D, D103C, and D103S) were successfully prepared using nondegenerate oligonucleotides, the overlap and extension method (*24*), and the polymerase chain reaction. Before mutagenesis, the *ccrA* gene was ligated into pUC19, and the resulting plasmid, pMSZ03, was used as the template in the PCR reactions. In our hands, the use of a pUC19-based plasmid as template, instead of the pET27b-based vector, resulted in >10-fold higher yields of PCR products, thus facilitating all subsequent subcloning steps. After mutagenesis and sequencing, the mutated gene was removed from the pMSZ03 and ligated into pET27b, and DNA sequencing of the entire *ccrA* gene in both directions was used to confirm that only the desired mutations were present. Protein overexpression and purification was performed utilizing the method of Wang and Benkovic (*18*), except in our studies, only one column (Q-Sepharose) was used to purify the protein samples, which were >95% pure as shown by SDS−PAGE. However, there was a slight brown coloration of the purified CcrA samples after Q-Sepharose chromatography. Since no protein bands >5000 Da were present in SDS−PAGE gels, we attribute this brown coloration to small peptides in the LB media that tightly adhere to CcrA. In the procedure of Wang and Benkovic (*18*), a second column (G-75) was used to further purify wild-type CcrA. Gel filtration chromatography was performed on several of our samples, but the purified protein samples showed no improvement in color quality and a substantial decrease in protein yield. Therefore, the final gel filtration chromatographic step was not included in the protein preparations described here.

Wild-type CcrA preparations yielded an average of 50 mg of active protein per liter of growth culture. SDS−PAGE gels of purified CcrA showed a single band at ca. 26 kDa, in agreement with earlier studies (*3, 18, 27*). The K184A, K184L, K184E, N193A, N193L, and N193D mutants were isolatable at levels comparable to those of wild-type CcrA. The D103C and D103S mutants were isolatable at levels half of that which was obtained for wild-type CcrA.

Circular dichroism spectra were collected on wild-type CcrA and CcrA mutants to ensure that CcrA expressed using the pET27b overexpression system had the correct secondary structure and that the point mutations did not cause a large change in the secondary structure of the enzyme. All of the mutants had CD spectra that were superimposable on that of wild-type CcrA (data not shown).

Metal Content of CcrA Mutants. Inductively coupled plasma spectrometry with atomic emission detection was used to determine the zinc content of wild-type CcrA and the CcrA mutants (Table 2). Wild-type CcrA was shown to contain 1.5 ± 0.1 mol of zinc per mole of protein, which is in agreement with values published by Rasmussen and co-workers (*28*) but lower than values published by others (*18, 29*). All of the mutants were shown to bind between 1.4 and 2.0 mol of zinc per mole of protein, which is comparable to the metal content of wild-type CcrA (Table 2).

Steady-State Kinetics. Steady-state kinetic studies were performed on multiple preparations of the wild-type CcrA and the CcrA mutants, and the resulting kinetic data are shown in Table 3. Wild-type CcrA exhibited k_{cat} values of 216 ± 13, 99 ± 2, and 54 ± 2 s^{-1} when using nitrocefin, penicillin G, and cephaloridine as substrates, respectively. The wild-type enzyme yielded K_m values of 7.8 ± 1.3, 50 ± 2, and 6.4 ± 0.9 μM when using nitrocefin, penicillin G, and cephaloridine as the substrates (Table 3). The inclusion of 100 μM $ZnCl_2$ to the assay buffer had no effect on the determined steady-state kinetic constants of wild-type CcrA or of any of the CcrA mutants.

The Lys184 mutants exhibited less than a 2-fold change in K_m, with values of 4.8 ± 0.2, 15 ± 2, and 4.2 ± 0.2 μM for the K184A, K184E, and K184L mutants, respectively, when using nitrocefin as the substrate (Table 3). When using cephaloridine as the substrate, these same three mutants showed less than 4-fold decrease in K_m, with the K184E mutant exhibiting the largest value for K_m (Table 3). However, when penicillin G is used as substrate, the K184A, K184E, and K184L mutants yielded markedly increased values for K_m as compared to wild-type CcrA, with a >10-fold increase for the K184L mutant, a >20-fold increase for the K184A mutant, and a 40-fold increase for the K184E mutant (Table 3). The Lys184 mutants also demonstrated small changes in k_{cat}, with a 2−4-fold decrease when using

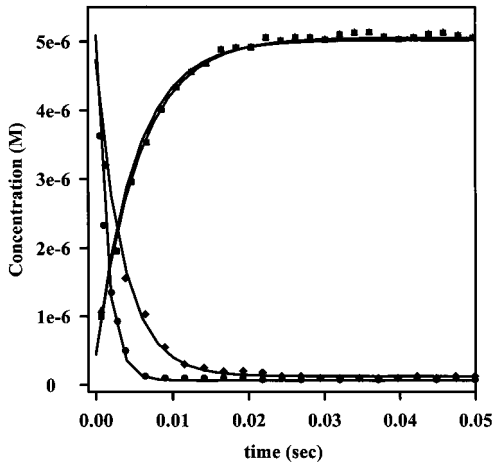

FIGURE 2: Stopped-flow Vis studies of wild-type CcrA and the N193A mutant with nitrocefin in 1× MTEN, pH 7.0. Substrate disappearance data for the reaction of 5 μM nitrocefin with 25 μM wild-type CcrA (●) and 25 μM N193A (◆) and product formation data for the reaction of 5 μM nitrocefin with 25 μM wild-type CcrA (■) and 25 μM N193A (▲) are shown. Absorbance data were converted to concentration data as described under Experimental Procedures. The data sets were fitted to exponential equations as described under Experimental Procedures.

nitrocefin as substrate and 2−4-fold increases when using penicillin G and cephaloridine as the substrate.

The Asn193 mutants yielded a 2−4-fold decrease in k_{cat} when using nitrocefin as the substrate; however, when using penicillin G and cephaloridine as substrates, 2−3-fold increases in k_{cat} were observed (Table 3). The observed changes in K_m values for the Asn193 mutants were mixed, with no significant change for the N193A and N193D mutants and a 3-fold increase in K_m for the N193L mutant when using nitrocefin as substrate. On the other hand, 3−9-fold increases in K_m were exhibited for the N193A and N193D mutants when using penicillin G or cephaloridine as the substrate, and greater than 10-fold increases in K_m for the N193L mutant when using the same substrates.

The Asp103 mutants exhibited significant decreases in k_{cat}, with values of <0.003 and 1.9 ± 0.1 s^{-1} for the D103S and D103C mutants, respectively. The observed K_m values for the D103C mutant were 2−6-fold higher than for wild-type CcrA.

Pre-Steady-State Kinetic Studies on the N193 Mutants of CcrA. Pre-steady-state kinetic studies were conducted on wild-type CcrA and the N193 mutants to evaluate the effect of the mutations on individual kinetic steps. The reaction of 25 μM wild-type CcrA with 5 μM nitrocefin resulted in the rapid disappearance of substrate (●) and rapid appearance of product (■) (Figure 2). Fitting these single-turnover data (*18*) to exponential equations resulted in rate constants of 790 ± 5 and 183 ± 5 s^{-1} for substrate disappearance and product formation, respectively. These values are very similar to those previously reported by Wang and Benkovic (*18*). The reaction of 25 μM N193A with 5 μM nitrocefin resulted in product formation data (▲) that were superimposable on the wild-type CcrA data (■) with a rate constant of 190 ± 3 s^{-1} (Figure 2). Similar plots were attainable using the N193D and N193L mutants and using higher concentrations of the N193 mutants, although greater than 50 μM N193L was required to observe a rate constant of 190 s^{-1} for this mutant (data not shown).

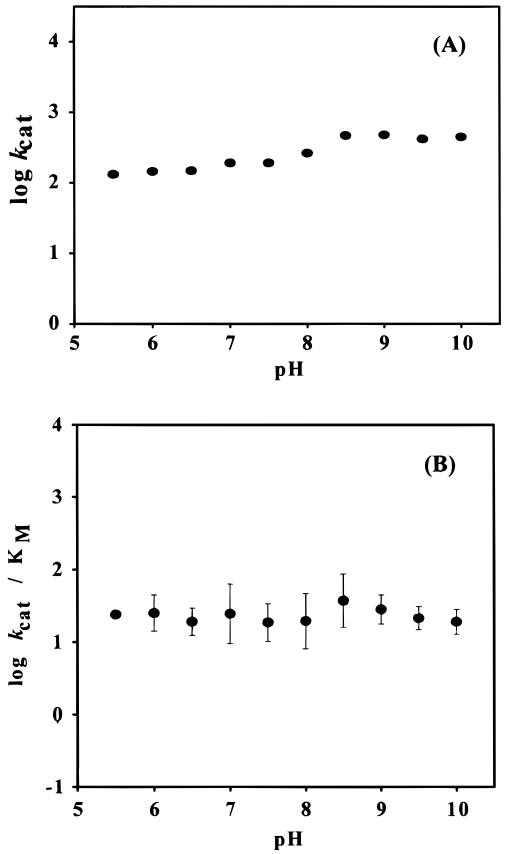

FIGURE 3: pH dependence of log k_{cat} (A) and log (k_{cat}/K_m) (B) for D103C CcrA-catalyzed hydrolysis of nitrocefin at 25 °C.

However, the rate of substrate disappearance was markedly slower for the N193 mutants. The reaction of 25 μM N193A with 5 μM nitrocefin resulted in substrate disappearance data (◆) that had a rate constant of 280 ± 6 s^{-1} (Figure 2). Similar plots were attainable using higher concentrations of N193A or using the N193D and N193L mutants (data not shown).

pH Dependence of Steady-State Kinetic Constants for the D103C and D103S Mutants. To further probe the role of Asp103 in the mechanism of CcrA, the pH dependence of the steady-state kinetic constants k_{cat} and k_{cat}/K_m was examined using wild-type CcrA and the D103C mutant and nitrocefin as the substrate. These studies were conducted in 1× MTEN over a pH range of 5.5−10, as described previously by Wang and Benkovic (*18*). In buffers with pH values less than 5.5, the enzyme and mutants precipitated, and at pH values greater than 10, the background hydrolysis of nitrocefin in the absence of enzyme was too fast to obtain meaningful data. Studies using wild-type CcrA yielded log k_{cat} and log (k_{cat}/K_m) versus pH plots that were flat in the pH range tested (data not shown). These plots are identical to those previously reported by Wang and Benkovic (*18*) and suggest that there are no ionizable groups with pK_a values between 5.5 and 10 involved in the rate-limiting step of nitrocefin hydrolysis by wild-type CcrA. When using the D103C mutant, log k_{cat} and log (k_{cat}/K_m) versus pH plots were observed that were also relatively flat and had no detectable inflections with unit changes in slope (Figure 3), indicating that this mutant, like wild-type CcrA, has no ionizable groups with pK_a values between 5.5 and 10.

Solvent Isotope Effects and Proton Inventories. Solvent isotope studies were conducted in 1× MTEN at pH 7.0 using

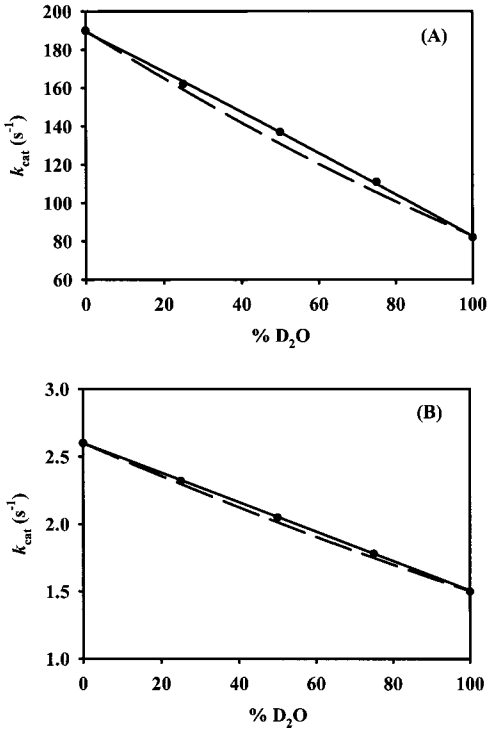

FIGURE 4: Proton inventory plots of nitrocefin hydrolysis at pH 7.0 by (A) wild-type CcrA and (B) D103C mutant. For these studies, the error bar for each data point is smaller than the data point symbol. The solid line (—) represents a single proton in flight model and was drawn from the equation: $k_{obs} = k_{cat}[1 - n + n(k^D/k^H)]$ as described under Experimental Procedures. The dashed line (– –) represents a two protons in flight model and was drawn from the equation: $k_{obs} = k_{cat}[1 - n + n(k^D/k^H)]^2$ (*31*). The two protons in flight model assumed that both protons had identical fractionation factors (*30*−*32*).

wild-type CcrA and the D103C mutant and nitrocefin as the substrate. Wild-type CcrA exhibited a solvent isotope effect of $k^H/k^D = 2.6 \pm 0.1$ and $(k^H/K_m^H)/(k^D/K_m^D) = 1.4 \pm 0.1$, which are values in excellent agreement with previously reported values (*18*). The D103C mutant exhibited a solvent isotope effect of $k^H/k^D = 1.8 \pm 0.1$ and $(k^H/K_m^H)/(k^D/K_m^D) = 1.3 \pm 0.1$, suggesting a proton transfer in a kinetically significant step of the reaction for both wild-type CcrA and the D103C mutant.

To address the number of proton transfers occurring in the kinetically significant step, proton inventory studies were conducted in 1× MTEN at pH 7.0 using nitrocefin as the substrate and wild-type CcrA and the D103C mutant. Plots of k_{cat} versus % D_2O were linear and best-fitted using a one proton in flight model, suggesting that one proton is in flight for wild-type CcrA (Figure 4A) (*30*−*32*). In the case of the D103C mutant, lines corresponding to a one proton and two protons in flight model are very similar; therefore, the possibility of two protons in flight during a rate-significant step(s) of the D103C mutant cannot unambiguously be ruled out (Figure 4B). By fitting the proton inventory data to $k_{obs} = k_{cat}[1 - n + n(k^D/k^H)]$, fractionation factors of 0.99 ± 0.1 and 0.91 ± 0.02 were determined for wild-type CcrA and the D103C mutant, respectively.

Rapid-Scanning Visible Studies on the D103C Mutant of CcrA. Rapid-scanning Vis studies were conducted to establish whether the reaction intermediate that absorbs at 665 nm could be detected using the D103C mutant. The reaction of various concentrations of wild-type CcrA and nitrocefin

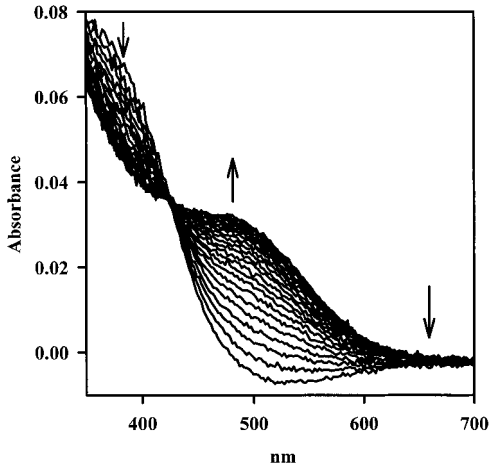

FIGURE 5: Rapid-scanning Vis spectra of the reaction of 100 μM D103C and 5 μM nitrocefin in 1× MTEN buffer, pH 7.0, at 25 °C.

resulted in three prominent features: (1) a peak at 390 nm which disappeared quickly, (2) a peak at 485 nm which increased in intensity during the reaction, and (3) a peak at 665 nm which reached a maximum absorbance during the first few milliseconds of the reaction and disappeared during the remainder of the reaction (data not shown). These features are attributed to substrate (390 nm), product (485 nm), and intermediate (665 nm), and similar rapid-scanning Vis spectra have been reported by Wang and Benkovic for wild-type CcrA (*18*−*20*).

The reaction of D103C at concentrations ranging from 25 to 200 μM and 5−100 μM nitrocefin was also probed by rapid-scanning Vis studies. Since the D103C mutant exhibits k_{cat} values 10^2 lower than wild-type CcrA, the reaction was monitored for 2 s to ensure that the reaction had proceeded to completion. The reaction of 100 μM D103C and 5 μM nitrocefin resulted in spectra with only two features: (1) a peak at 390 nm that lost intensity during the course of the reaction and (2) a peak at 485 nm that increased in intensity during the reaction (Figure 5). In none of the reactions tested were we able to detect the presence of the intermediate that absorbs at 665 nm.

DISCUSSION

Previous biochemical, kinetic, and structural studies have indicated significant differences among the metallo-β-lactamases (*1*, *11*, *21*, *33*, *34*). These differences suggest that one inhibitor may not inhibit all metallo-β-lactamases; in fact, previous studies using nonclinical inhibitors have shown widely different effacacies and interactions of the inhibitors with the different metallo-β-lactamases (*12*, *13*, *16*, *17*, *35*−*38*). The published crystal structures of CcrA, L1, and β-lactamase II demonstrate different active site amino acids, and computer modeling studies using these crystal structures as a basis have been used to predict distinct substrate binding models and reaction mechanisms (*4*, *5*, *9*). Structural and mechanistic studies have been used to propose a reaction mechanism for the metallo-β-lactamase CcrA from *B. fragilis* that involves a kinetically significant proton transfer, a role of Lys184 in substrate binding, and a role of Asn193 in catalysis (*18*−*21*). The focus of this work is to probe the proposed roles of Lys184 and Asn193 by generating and

characterizing site-directed mutants of CcrA, as well as testing whether Asp103 takes part in the rate-limiting proton transfer.

By using the procedure of Wang and Benkovic, active, soluble CcrA can be isolated at levels comparable to those previously reported (*18*). Using the pET27b-overexpressed wild-type CcrA and nitrocefin as substrate, Wang et al. reported K_M and k_{cat} values of 7.1 μM and 226 s^{-1}, respectively (*18*). In our hands, wild-type CcrA exhibits steady-state kinetic constants identical within error to those previously published. However, Paul-Soto et al. reported k_{cat} values for nitrocefin hydrolysis by CcrA with two Zn(II) ions to be 260 s^{-1} (*39*). Several values for the steady-state kinetic constants when using penicillin G as substrate have been reported (*3, 4, 27, 28, 39*): K_m values have been reported to range between 8 and 97 μM, and k_{cat} values range from 94 to 247 s^{-1}. A similar range of steady-state kinetic constants have been reported for metallo-β-lactamase from *B. fragilis* when using cephaloridine as substrate (*3, 27, 28, 39*): K_m values ranging from 2.8 to 12 μM and k_{cat} values ranging from 20 to 73 s^{-1}. Generally, the K_m values determined in this study agree nicely with those previously reported, and the k_{cat} values reported are slightly less than previously reported. The metal content reported here for wild-type CcrA (Table 2) was found to be approximately 0.5 mol of Zn(II)/mol of protein less than previously published (*4, 18, 29, 40*).

These discrepancies in metal content and k_{cat} values can be explained by the presence of a faint, persistent coloration of purified CcrA samples. The absorbance of CcrA at 280 nm was used to calculate the concentration of the enzyme samples (*18*). It is possible that the species in the CcrA samples that resulted in the brownish tint absorbed at 280 nm, thus leading to higher predicted enzyme concentrations, lower k_{cat} values, and lower metal to enzyme stoichiometries. The fact that adding Zn(II) in the assay buffers does not lead to an increase in k_{cat} supports this explanation for the observed low metal:enzyme stoichiometries and k_{cat} values and indicates that the CcrA samples isolated in this study bind their full complement of Zn(II). The species giving rise to the brownish tint are low molecular weight compounds because they are undetectable in SDS−PAGE gels and are most likely peptides from the LB growth media. Unfortunately, these contaminants could not be removed from CcrA samples using Sephacryl S-200 or G-75 gel filtration chromatographies.

The lysine residue at position 184 is conserved in all sequenced metallo-β-lactamases except L1 from *S. maltophilia* (*1, 11, 21, 34*). Lys184 is proposed to aid in the binding of substrate within the active site of CcrA by forming a salt bridge with the invariant carboxylate on the five- or six-membered ring of the β-lactam-containing antibiotics (*4*). In support of this proposed role, the crystal structure of metallo-β-lactamase from *B. fragilis* with a bound biphenyltetrazole (competitive inhibitor) demonstrated that Lys184 interacts via a water molecule with the inhibitor (*15*). In addition, the sulfonic acid oxygens on the weak competitive inhibitor MES were shown to interact with Lys184 (*14*). If the role of this residue is as previously proposed, a substitution of lysine with a negatively charged or uncharged residue should dramatically increase the Michaelis constant, which is, to a first approximation, a measure of how tightly substrates are bound within the active site (*41*).

To probe the role of Lys184 in substrate binding, three mutants of CcrA were generated and characterized: (a) lysine was changed to a small, uncharged alanine (K184A); (b) lysine was changed to a larger, uncharged leucine (K184L); and (c) lysine was changed to a negatively charged glutamate (K184E). CD spectra of the Lys184 mutants showed no changes in the secondary structure of the mutants as compared to those of wild-type CcrA (data not shown), and metal analyses of the Lys184 mutants demonstrated that these mutants bind the same stoichiometry of Zn(II) as wild-type CcrA (Table 2). These two pieces of evidence suggest that no major structural changes in the enzymes occurred with the point mutations. When using cephalosporins as the substrates, the replacement of the positively charged lysine with the uncharged residues resulted in K184A and K184L mutants that exhibited less than 3-fold changes in K_M values as compared to wild-type CcrA (Table 3). The replacement of lysine with a negatively charged residue resulted in the K184E mutant that had only a 2-fold or 4-fold higher K_M value for nitrocefin or cephaloridine binding, respectively, than wild-type CcrA. These results on the Lys184 mutant argue against the proposed substrate-binding role of Lys184 to cephalosporins. On the other hand, Lys184 does appear to have a role in substrate binding to penicillin G. The K184A, K184E, and K184L mutants exhibited 20-fold, >75-fold, and 12-fold increases in K_m, respectively. The relatively higher K_m for the K184E mutant supports the proposed interaction of Lys184 with the invariant carboxylate on penicillins. The difference in CcrA's interaction with cephalosporins and penicillins is not surprising. The carboxylate on the five-membered ring of penicillin G is bonded to a carbon that is sp^3 hybridized; therefore, the carboxylate would be pointing away from the β-lactam carbonyl. On the other hand, the carboxylate on the six-membered ring of nitrocefin and cephaloridine is sp^2 hybridized and is better aligned with the β-lactam carbonyl. Mobashery and co-workers used a similar argument to explain the differential binding of penicillins and cephalosporins to TEM-1 (*42, 43*).

The asparagine at position 193 is invariant in all sequenced metallo-β-lactamases except in BlaB and IND-1 from two *Chryseobacterium* strains (*44, 45*). Previous crystallographic and modeling studies on CcrA have implicated the amine group of asparagine at position 193 and Zn_1 in polarizing the carbonyl group on the substrate (*4*). In addition, it has been proposed that the oxyanion hole formed by Zn_1 and Asn193 stabilizes the charges within the active site as the intermediate forms and decays during hydrolysis (*21*). In support of these roles, crystal structures of competitive inhibitors bound to metallo-β-lactamase from *B. fragilis* have demonstrated that Asn193 forms a H-bond with inhibitors (*14, 15*).

To probe the proposed role of Asn193, three site-directed mutants were generated and characterized: (a) asparagine replaced with a small, nonpolar alanine (N193A); (b) asparagine replaced with a larger, nonpolar leucine (N193L); and (c) asparagine replaced with a negatively charged aspartic acid (N193D). CD spectra of the three purified mutants showed no significant secondary structure changes resulting from the point mutations as compared to wild-type CcrA (data not shown). Metal analyses on the mutants showed that the point mutations did not adversely affect metal binding as compared with wild-type CcrA (Table 2).

Steady-state kinetic studies were conducted on the N193A, N193D, and N193L mutants using nitrocefin, penicillin G, and cephaloridine as the substrate. When using penicillin G or cephaloridine as substrate, there was a 3−9-fold increase in K_m for the N193A and N193D mutants, and a >15-fold increase in K_m for the K193L mutant. A much smaller change in K_m was observed for these mutants using nitrocefin as the substrate; however, the largest K_m value for nitrocefin was also exhibited by the N193L mutant. The relatively larger K_m values for the N193L mutant can be explained by the increased steric bulk of leucine's side chain as compared to asparagine, aspartic acid, or alanine side chains. The smaller observed changes in K_m for the Asn193 mutants when using nitrocefin may be due to larger substituents on nitrocefin as compared to penicillin G and cephaloridine, and CcrA's ability to accommodate for the loss of Asn193/substrate interaction with other protein/substrate interactions. No matter which substrate was used, there was < 4-fold change in k_{cat} (Table 3), suggesting that either Zn_1 can accommodate for the loss of the Asn193 interaction with substrate or that Asn193 is not playing a large role in substrate activation (*4, 21*).

However, we wondered if the effects of the N193 mutations were masked as the rate of product formation has been reported to be over 10 times lower than the rate of substrate disappearance for wild-type CcrA (*18*−*20*). The k_{cat} values are determined by using an assay where product formation is followed over time (*25*); if the N193 mutations affected a step preceding product formation, a large change in k_{cat} would not be expected. Therefore, stopped-flow Vis studies were conducted on the N193 mutants (Figure 2). The Asn193 mutations did not affect the rate of product formation but did result in ca. 3-fold drop in the rate of substrate disappearance. These results suggest that Asn193 takes part in substrate binding and catalysis as previously predicted (*4, 21*), although Zn(II) and possibly other active site residues can partially accommodate for the loss of Asn193.

The proposed mechanism for the hydrolysis of β-lactam-containing antibiotics by CcrA distinguishes Asp103 as significant (*4*). Crystallographic data by Concha and co-workers suggest that Asp103 forms an electrostatic interaction with the water/hydroxide bridging the two active site Zn(II) ions (*4*). This residue orients the Zn_1−OH species so as to initiate its nucleophilic attack on the substrate. Asp103 was also postulated to control the bond strength between Zn_2 and the bridging hydroxide (*21*). Given the position of the unligated oxygen of Asp103, it is also likely that this residue may accept a proton from the bridging water/hydroxide molecule and/or transfer a proton to the intermediate during the rate-limiting step to form the product (*11*). Recently, Diaz et al. used computational studies to show how the interaction of Asp103 with the bridging hydroxide/water nicely explains the inability to observe inflection points in pH dependence plots (*46*).

To probe the role of Asp103, the aspartic acid was replaced with cysteine and serine to create the D103C and D103S mutants, respectively. Although these mutants were isolatable at levels half that of wild-type CcrA, metal analyses demonstrated that the D103S and D103C mutants bind the same amount of Zn(II) as wild-type CcrA (Table 2), and CD spectra of the mutants are superimposable over those of wild-type CcrA. The former result suggests that cysteine and serine can serve as metal-binding ligands in these CcrA mutants, or that the other metal-binding ligands to Zn_2 can compensate for the loss of one metal ligand. In contrast to this latter possibility are the previous reports that the D103V and D103N mutants do not bind their full complement of Zn(II) (*28, 29*).

The D103C mutant exhibited a 2−6-fold increase in K_m for the substrates tested, which is similar to increases previously reported (*28, 29*). However, Yang et al. reported that the affinity for imipenem increased (10-fold lower K_m) for the D103N mutant (*28*). In our hands, the K_m values for imipenem using wild-type CcrA or any of the mutants tested were >200 μM. Attempts to conduct assays with wild-type CcrA or any mutant and >500 μM imipenem resulted in significant substrate inhibition, an inability to saturate the enzymes, and an inability to accurately determine k_{cat} or K_m for this substrate (Crowder, unpublished results).

Both Asp103 mutants exhibited a significant decrease in hydrolytic activity, with the D103C mutant exhibiting a 10^2-fold decrease and the D103S mutant exhibiting a greater than 10^5-fold decrease in k_{cat} as compared to the activity of wild-type CcrA (Table 3) when using nitrocefin as the substrate. Similar reductions in k_{cat} were observed when using penicillin G or cephaloridine as the substrate (Table 3). Similar decreases in k_{cat} were also previously reported for a D103V mutant of CcrA (*29*). The large difference in k_{cat} values between the D103S and D103C mutants may be explained by the differing metal environments in the two mutants. Wang et al. and Diaz et al. have predicted that the precise electronic properties of Zn_2 are critical for catalysis, and the data from these Asp103 mutants support this prediction (*20, 46*). Recently, Yang et al. have suggested, based on the small, 2-fold decrease in k_{cat} for a D103N mutant of CcrA when using imipenem as the substrate (see above), that D103 does not take part in catalysis and only serves to bind Zn(II) (*28*). Nonetheless, significant decreases in k_{cat} were observed using cephaloridine and penicillin G as substrates and the D103N mutant (*28*). Given that both D103S and D103C bind similar stoichiometries of Zn(II) as wild-type CcrA (Table 2), our data indicate that Asp103 does play a significant role in catalysis.

Wang and Benkovic have recently proposed that the rate-limiting step for nitrocefin hydrolysis is protonation of the intermediate to form product (*20, 21*). Proton inventory (Figure 3A) and solvent isotope studies using nitrocefin as the substrate and wild-type CcrA support this proposed mechanism. The significantly reduced k_{cat} values of the Asp103 mutants suggest that the proton that is transferred to the intermediate to form the product originates from Asp103. A proton on Asp103 is expected to have a pK_a lower than 5.0, which nicely explains why no inflection points are observed in pH dependence plots of nitrocefin hydrolysis by wild-type CcrA. However, rapid-scanning Vis studies on D103C and nitrocefin indicate that the D103C mutant does not utilize a mechanism where an intermediate is formed and the decay of that intermediate is rate-limiting (Figure 5).

A reaction mechanism accounting for previous mechanistic and structural studies (*4, 15, 18*−*21*), the recent computational studies (*46*), and the results in this work is shown in Figure 6. The resting form of the enzyme at pH 7.0 has a terminally bound water on Zn_2 and a bridging hydroxide

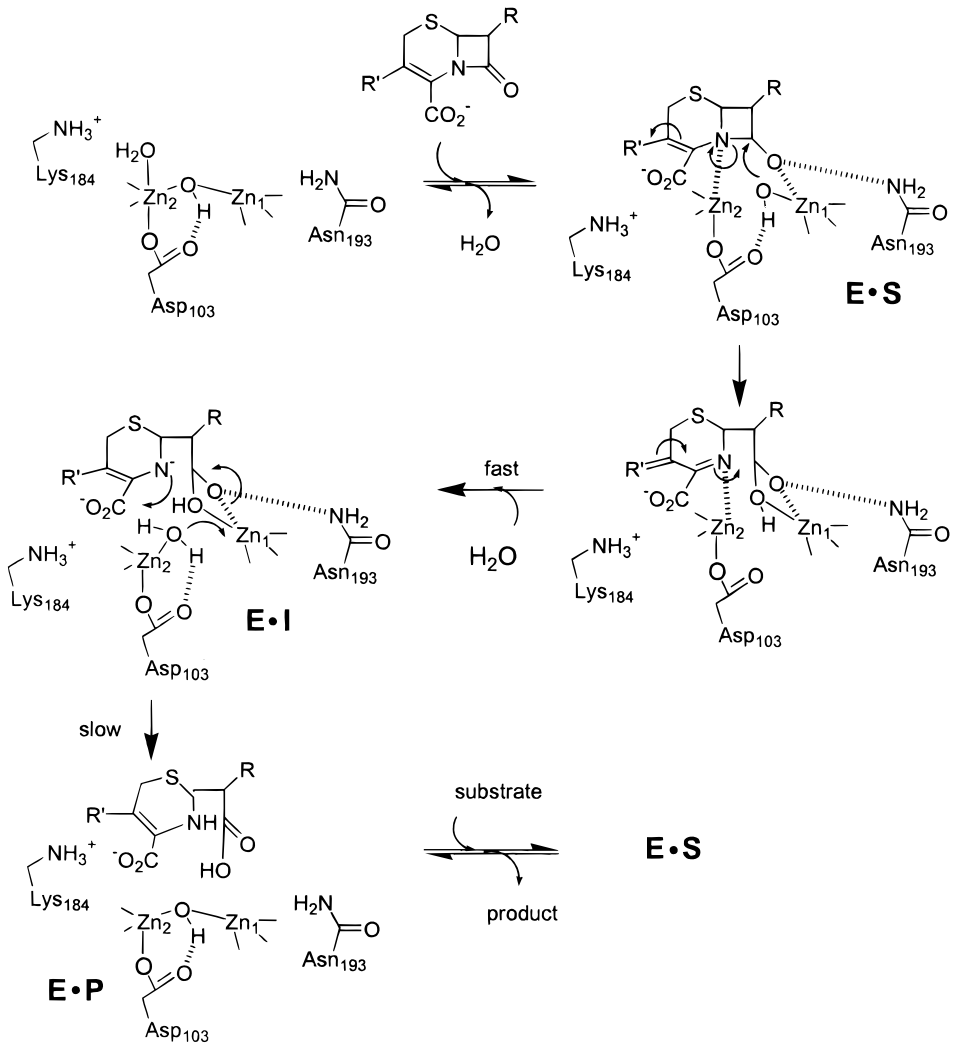

FIGURE 6: Proposed reaction mechanism for metallo-β-lactamase CcrA from *Bacteroides fragilis*.

which is H-bonded to Asp103. The binding of penicillin has the β-lactam carbonyl interacting with Zn_1 and Asn193 and the β-lactam nitrogen interacting with Zn_2. Since the substrate used in Figure 6 is nitrocefin, no contact between Lys184 and substrate carboxylate is shown. Zn_1 and Asn193, acting as Lewis acids, polarize the carbonyl bond on the substrate, making the carbonyl carbon more susceptible to nucleophilic attack. The nucleophile, formerly the bridging hydroxide, is oriented by Asp103 for attack. The proposed roles for Lys184 and Asn193 are supported by the data in this work. The substrate proceeds through a short-lived, tetrahedral transition state into the intermediate (E·I) (*19*, *21*, *46*). Wang et al. have demonstrated that the rate-limiting step for wild-type CcrA is breakdown (protonation) of this intermediate (*20*). The data presented in this work support the proposal (*4*, *21*) that the proton in flight originates from solvent rather than from Asp103. If Asp103 is the proton donor to the intermediate, then cysteine or serine would be the proton donor in the D103C and D103S mutants, respectively. The value of the fractionation factors in the proton inventory studies argues against the involvement of an −S−H group (*31*). Since the rapid-scanning studies showed that D103C utilizes a different rate-limiting step than wild-type CcrA despite having nearly identical pH dependence and solvent isotope effects, the role of Asp103 is most likely to aid in the formation and orientation of the nucleophile for attack on substrate. In wild-type CcrA, Asp103 aids in the deprotonation of the water or orientation of the hydroxide during the relatively fast second step (k_2) and apparently in the deprotonation of the incoming water/protonation of the intermediate during the slow step (k_3). This role is supported by solvent isotope studies which suggest a rate-significant proton transfer, pH dependence studies which suggest that the proton arises from a group with a pK_a of <5.0, and proton inventory studies which indicate a single proton with a fractionation factor of ca. 1.0 (i.e., a −O−H) (*30*−*32*). A water bridging two Zn(II) ions with an aspartic acid acting as an internal acid would result in a proton with a pK_a under 5.0 (*46*). The absence of an inflection point in the pH dependence plots of wild-type CcrA argues against the proton arising from a terminally bound water, although this possibility cannot be completely ruled out (expected pK_a of 7−8). The data presented here do not rule out the possibility of an enzyme group with a pK_a >10 serving as the proton donor.

For the D103C mutant, the similar pH dependence plots and proton inventory results (including the value of the fractionation factor) suggest a similar solvent derived proton with a pK_a of <5.0 in a rate-significant step. However, the inability to detect an intermediate in rapid-scanning studies suggests a different rate-determining step where deprotonation of the ultimate nucleophile is rate-limiting. It is not clear

why an aspartic acid is necessary to aid in the deprotonation of a water bridging between two Zn(II) ions, since the first pK_a of the bridging water should be under 6.0 (*46, 47*).

The results presented here further elucidate the role of conserved active site residues in the binding of substrate and the catalytic mechanism. This information can now be compared to similar studies on metallo-β-lactamases from the other subgroups, and the comparisons can possibly be used to identify common binding and mechanistic aspects of the enzymes which can be targeted for the generation of potential inhibitors.

ACKNOWLEDGMENT

We thank Dr. Beth Rasmussen of Wyeth-Ayerst (Lederle Laboratories) for sharing the original *CcrA* gene with us, and Drs. Walt Fast and Zhigang Wang for sharing the pMSZ02 plasmid, reading the manuscript, and helpful suggestions and comments. We thank Professor Russ Hille of The Ohio State University for the use of his stopped-flow instrument and Professor Ken Blumenthal of the University of Cincinnati for the use of his CD spectropolarimeter.

REFERENCES

1. Bush, K. (1998) *Clin. Infect. Dis. 27 (Suppl. 1)*, S48−53.
2. Payne, D. J. (1993) *J. Med. Microbiol. 39*, 93−99.
3. Yang, Y., Rasmussen, B. A., and Bush, K. (1992) *Antimicrob. Agents Chemother. 36*, 1155−1157.
4. Concha, N. O., Rasmussen, B. A., Bush, K., and Herzberg, O. (1996) *Structure 4*, 823−836.
5. Fabiane, S. M., Sohi, M. K., Wan, T., Payne, D. J., Bateson, J. H., Mitchell, T., and Sutton, B. J. (1998) *Biochemistry 37*, 12404−12411.
6. Orellano, E. G., Girardini, J. E., Cricco, J. A., Ceccarelli, E. A., and Vila, A. J. (1998) *Biochemistry 37*, 10173−10180.
7. Valladares, M. H., Felici, A., Weber, G., Adolph, H. W., Zeppezauer, M., Rossolini, G. M., Amicosante, G., Frere, J. M., and Galleni, M. (1997) *Biochemistry 36*, 11534−11541.
8. Felici, A., Perilli, M., Fransceschini, N., Rossolini, G. M., Galleni, M., Frere, J. M., Oratore, A., and Amicosante, G. (1997) *Antimicrob. Agents Chemother. 41* (4), 866−868.
9. Ullah, J. H., Walsh, T. R., Taylor, I. A., Emery, D. C., Verma, C. S., Gamblin, S. J., and Spenser, J. (1998) *J. Mol. Biol. 284*, 125−136.
10. Crowder, M. W., Walsh, T. R., Banovic, L., Pettit, M., and Spencer, J. (1998) *Antimicrob. Agents Chemother. 42* (4), 921−926.
11. Crowder, M. W., and Walsh, T. R. (1999) *Research Signpost 3*, 105−132.
12. Payne, D. J., Bateson, J. H., Gasson, B. C., Proctor, D., Khushi, T., Farmer, T. H., Tolson, D. A., Bell, D., Skett, P. W., Marshall, A. C., Reid, R., Ghosez, L., Combret, Y., and Marchand-Brynaert, J. (1997) *Antimicrob. Agents Chemother. 41*, 135−140.
13. Payne, D. J., Bateson, J. H., Gasson, B. C., Khushi, T., Proctor, D., Pearson, S. C., and Reid, R. (1997) *FEMS Microbiol. Lett. 157*, 171−175.
14. Fitzgerald, P. M. D., Wu, J. K., and Toney, J. H. (1998) *Biochemistry 37*, 6791−6800.
15. Toney, J. H., Fitzgerald, P. M. D., Grover-Sharma, N., Olson, S. H., May, W. J., Sundelof, J. G., Vanderwall, D. E., Cleary, K. A., Grant, S. K., Wu, J. K., Kozarich, J. W., Pompliano, D. L., and Hammond, G. G. (1998) *Chem. Biol. 5*, 185−196.
16. Scrofani, S. D. B., Wright, P. E., and Dyson, H. J. (1998) *Protein Sci. 7*, 2476−2479.
17. Scrofani, S. D. B., Chung, J., Huntley, J. J. A., Benkovic, S. J., Wright, P. E., and Dyson, H. J. (1999) *Biochemistry 38*, 14507−14514.
18. Wang, Z., and Benkovic, S. J. (1998) *J. Biol. Chem. 273*, 22402−22408.
19. Wang, Z., Fast, W., and Benkovic, S. J. (1998) *J. Am. Chem. Soc. 120*, 10788.
20. Wang, Z., Fast, W., and Benkovic, S. J. (1999) *Biochemistry 38*, 10013−10023.
21. Wang, Z., Fast, W., Valentine, A. M., and Benkovic, S. J. (1999) *Curr. Opin. Chem. Biol. 3*, 614−622.
22. Rasmussen, B. A., Gluzman, Y., and Tally, F. P. (1990) *Antimicrob. Agents Chemother. 34*, 1590−1592.
23. Sambrook, J., Fritsch, E. F., and Maniatis, T. (1989) *Molecular Cloning—A Laboratory Manual*, 2nd ed., Vol. 3, Cold Spring Harbor Laboratory Press, Cold Spring Harbor, NY.
24. Ho, S. N., Hunt, H. D., Horton, R. M., Pullen, J. K., and Pease, L. R. (1989) *Gene 77*, 51−59.
25. O'Callaghan, C. H., Morris, A., Kirby, S. M., and Shingler, A. H. (1972) *Antimicrob. Agents Chemother. 1*, 283−288.
26. McMannus-Munoz, S., and Crowder, M. W. (1999) *Biochemistry 38*, 1547−1553.
27. Toney, J. H., Wu, J. K., Overbye, K. M., Thompson, C. M., and Pompliano, D. L. (1997) *Protein Expression Purif. 9*, 355−362.
28. Yang, Y., Keeney, D., Tang, X. J., Canfield, N., and Rasmussen, B. A. (1999) *J. Biol. Chem. 274*, 15706−15711.
29. Crowder, M. W., Wang, Z., Franklin, S. L., Zovinka, E. P., and Benkovic, S. J. (1996) *Biochemistry 35*, 12126−12132.
30. Venkatasubban, K. S., and Schowen, R. L. (1984) *CRC Crit. Rev. Biochem. 17*, 1−44.
31. Schowen, K. B. J. (1978) in *Transition States of Biochemical Processes* (Gandour, R. D., and Schowen, R. L., Eds.) pp 225−283, Plenum Press, New York.
32. Schowen, K. B., and Schowen, R. L. (1982) *Methods Enzymol. 87*, 551−606.
33. Cricco, J. A., Orellano, E. G., Rasia, R. M., Ceccarelli, E. A., and Vila, A. J. (1999) *Coord. Chem. Rev. 190−192*, 519−535.
34. Cricco, J. A., and Vila, A. J. (1999) *Curr. Pharm. Des. 5*, 915−927.
35. Felici, A., Perilli, M., Segatore, B., Franceschini, N., Setacci, D., Oratore, A., Stefani, S., Galleni, M., and Amicosante, G. (1995) *Antimicrob. Agents Chemother. 39*, 1300−1305.
36. Gilpin, M. L., Fulston, M., Payne, D., Cramp, R., and Hood, I. (1995) *J. Antibiot. 48*, 1081−1085.
37. Yang, K. W., and Crowder, M. W. (1999) *Arch. Biochem. Biophys. 368*, 1−6.
38. Bounaga, S., Laws, A. P., Galleni, M., and Page, M. I. (1998) *Biochem. J. 331*, 703−711.
39. Paul-Soto, R., Hernandez-Valladares, M., Galleni, M., Bauer, R., Zeppezauer, M., Frere, J. M., and Adolph, H. W. (1998) *FEBS Lett. 438*, 137−140.
40. Carfi, A., Paul-Soto, R., Martin, L., Petillot, Y., Frere, J. M., and Dideberg, O. (1997) *Acta Crystallogr., Sect. D D53*, 485−487.
41. Fersht, A. (1985) *Enzyme Structure and Mechanism*, 2nd ed., W. H. Freeman and Co., New York.
42. Zafaralla, G., Manavathu, E. K., Lerner, S. A., and Mobashery, S. (1992) *Biochemistry 31*, 3847−3852.
43. Imtiaz, U., Manavathu, E. K., Lerner, S. A., and Mobashery, S. (1993) *Antimicrob. Agents Chemother. 37*, 2438−2442.
44. Rossolini, G. M., Franceschini, N., Riccio, M. L., Mercuri, P. S., Perilli, M., Galleni, M., Frere, J. M., and Amicosante, G. (1998) *Biochem. J. 332*, 145−152.
45. Bellais, S., Leotard, S., Poirel, L., Naas, T., and Nordmann, P. (1999) *FEMS Microbiol. Lett. 171*, 127−132.
46. Diaz, N., Suarez, D., and Merz, K. M. (2000) *J. Am. Chem. Soc. 122*, 4197−4208.
47. Page, M. I., and Laws, A. P. (1998) *J. Chem. Soc., Chem. Commun.*, 1609−1617.

BI0010524